Astrophys Space Sci (2009) 323: 135–145
DOI 10.1007/s10509-009-0055-1

ORIGINAL ARTICLE

On properties of narrow CMEs observed with SOHO/LASCO

Nishant Mittal · Kumud Pandey · Udit Narain · S.S. Sharma

Received: 8 October 2008 / Accepted: 16 June 2009 / Published online: 2 July 2009

Abstract We have investigated properties such as speed, angular width, location, acceleration and occurrence rate of narrow CMEs (defined as having angular width $\leq 20°$) observed during 1996–2007 by SOHO/LASCO. The results obtained are compared with those of normal CMEs (angular width $> 20°$) from the same time interval to find whether there are any real differences between the two populations. Our study of 3464 narrow CMEs from the online SOHO/LASCO, CME catalogue leads us to conclude that (1) the fraction of narrow CMEs during solar minimum is 38% and during solar maximum 19%, (2) during solar maximum narrow CMEs are generally faster than normal CMEs, (3) the maximum speed of narrow CMEs is much smaller than that of the normal CMEs, (4) during solar maximum narrow CMEs appear at all latitudes similar to normal CMEs, (5) narrow and normal CMEs have unequal deceleration and (6) the occurrence rate of narrow CMEs remain constant after 1998 until the beginning of 2006 while the normal CMEs occurrence rate seems to follow solar cycle variation until 2004. Thus narrow CMEs and normal CMEs have some differences, in disagreement with previous studies.

Keywords Sun · Coronal mass ejections · Narrow CMEs · Solar cycle 23

N. Mittal (✉) · K. Pandey · U. Narain · S.S. Sharma
Astrophysics Research Group, Meerut College, Meerut 250001, India
e-mail: nishantphysics@yahoo.com

N. Mittal · U. Narain
IUCAA, Post Bag 4, Ganeshkhind, Pune 411007, India

1 Introduction

Coronal mass ejections (CMEs) were first detected in the 1970s by the Orbiting Solar Observatory (OSO-7) on 1971 Dec. 14 (Tousey 1973). Since their discovery CMEs have been observed by several space-borne instruments, namely the seventh Orbiting Solar Observatory (OSO-7) coronagraph, the Apollo Telescope Mount (ATM) coronagraph on board Skylab, the Solwind coronagraph on board the P78-1 satellite, the Coronagraph/Polarimeter (CP) on board Solar Maximum Mission (SMM), the Large Angle and Spectrometric Coronagraph (LASCO) on board the Solar and Heliospheric Observatory (SOHO), and Sun Earth Connection Coronal and Heliospheric Investigation (SECCHI) on board Solar Terrestrial RElations Observatory (STEREO). The ground-based instruments, e.g. the Mauna Loa K-Coronameter, have also observed CMEs. For more than three decades, the identification of the CMEs has been carried out by human eye and the event catalogs have been compiled manually (e.g. Howard et al. 1985; St. Cyr and Burkepile 1990; Burkepile and St. Cyr 1993; Yashiro et al. 2004; Gopalswamy et al. 2009). An automatic catalogue CACTus of CMEs is now available (Robbrecht et al. 2009).

CMEs are eruptions of plasma from the Sun that range in speed from 10 km/s to more than 3300 km/s (Gopalswamy 2004; Yashiro et al. 2004; Mittal et al. 2009). These solar phenomena are episodic expulsions of mass and magnetic field from the solar corona, which involve large scale reconfigurations of the corona and significant disturbances in the solar wind. Changes in the large scale coronal structure caused by mass ejections typically occur on timescales ranging from several minutes to several hours (Hundhausen et al. 1994) and are associated with solar wind disturbances that typically reach Earth in 3–4 days.

Since its launch in 1996, the number of CMEs detected by SOHO/LASCO exceeds more than 12000. The median apparent angular width of CMEs observed in the LASCO field of view is about 50° (St. Cyr et al. 2000), but the values have a broad distribution. CMEs with maximum apparent width of 360° are commonly known as Halo CMEs and are very important for space weather applications (Gopalswamy et al. 2000; St. Cyr et al. 2000; Webb et al. 2000; Gopalswamy 2006). CMEs with apparent angular width $\leq 20°$ are taken as narrow CMEs here.

Gopalswamy et al. (2002) suggested that only fast and wide CMEs have an important role in the production of large solar energetic particles (SEPs). Kahler et al. (2001) reported that some impulsive SEP events were also associated with fast but narrow CMEs. Narrow CMEs also may have an important role in impulsive SEP production or propagation into the interplanetary medium, and therefore it is important to understand the characteristics and origin of narrow CMEs.

Many CMEs originate from the disruption of a helmet streamer (Hundhausen 1993; Illing and Hundhausen 1986). When viewed near the solar limb such CMEs typically have a form characterized by a bright leading shell of material surrounding a dark cavity within which an erupted prominence is found (Crifo et al. 1983; Hundhausen 1987).

Burkepile and St. Cyr (1993) categorized CMEs using images taken by the SMM coronagraph based on of geometric characteristics exhibited by them. Their list consisted of the following categories: loop/cavity/core, mound, blob, jet, tongue and fan. CMEs listed by Munro and Sime (1985) from Skylab results are classified as loop, filled bottle, streamer separation, material injected into streamer, ray and cloud. CME classes listed by Howard et al. (1985) from P78-1 observations are loop, curved front, halo, spike, double spike, multiple spike, streamer blowout, fan and complex.

Wang et al. (1998) investigated the solar surface counterparts of 27-jet-like CMEs (having typical widths of $\sim 2°$–$4°$) observed above the polar coronal holes in the region 2.9–3.7 solar radii (R_S), using the EUV Imaging Telescope (EIT) on board SOHO and found that these particular type of narrow CMEs were the outward extensions of EUV jets (see also, Wang and Sheeley 2002). They also found that the leading edges of jet-like CMEs propagate at speeds of 400–1100 km/s, while the bulk of their material travels at around 250 km/s. Gilbert et al. (2001) examined properties of 15 narrow CMEs and found that their apparent speeds ranged from 159–630 km/s. They also investigated their surface associations and found that most narrow CMEs originate near a relatively sharp bend in a polarity-reversal line. They concluded that there is no obvious difference between the narrow and normal CMEs other than their appearance.

Normal CMEs are likely to have the well known three-part structure and can be explained as resulting from the expansion of flux tubes. Whether narrow CMEs differ morphologically from normal CMEs (Gilbert et al. 2001) is still unclear. Gilbert et al. (2001) suggested that narrow CMEs have no visible internal structure; it is also possible that some narrow CMEs do contain visible structure but the resolution of the LASCO instrument limits our ability to observe it. In contrast, the narrow CMEs seem to be mass flows in vertical flux tubes (Yashiro et al. 2003).

Yashiro et al. (2003) investigated the properties of narrow CMEs and found that the population of narrow CMEs increased towards solar maximum. During solar minimum narrow CMEs originate from the equatorial region, while during solar maximum narrow CMEs are ejected from all latitudes like normal CMEs. They showed that the average speed of narrow CMEs increases from 300 km/s during solar minimum to 550 km/s at solar maximum.

Very narrow CMEs are a small subset of normal CMEs that previously have not been extensively studied. We focus on this subset in this paper. In this study, we present the speed, angular width, location, acceleration and occurrence rate of narrow CMEs and compare them with the properties of large, more typical CMEs, i.e. normal CMEs. Our main aim is to establish whether there are any real differences between the two populations.

2 Data

There are two different methods of CMEs detection and the respective catalogues are publicly available. The LASCO CME catalogue at http://cdaw.gsfc.nasa.gov/CME_list and the CACTus catalogue at http://sidc.oma.be/cactus. The CDAW is a manual catalogue while CACTus is an automatic catalogue.

Over the past 12-years the SOHO/LASCO instrument has been detecting CMEs. The LASCO instrument (Brueckner, 1995) consists of three coronagraphs C1, C2 and C3 that span the fields of view 1.1–3R_S, 2–6R_S and 4–30R_S, respectively. Both C2 and C3 are externally occulted white-light coronagraphs; while C1 was designed for spectrometric purposes but has been out of operation since 1998 June (Wang and Sheeley 2002). A 3 month data gap occurred in 1998 from 24 June to 22 October due to an unexpected loss of contact with the spacecraft. Subsequent failure of all three gyroscopes caused an interruption from 21 December 1998 to 6 February 1999. A third data gap occurred in June 2003, when SOHO's main antenna became stuck. This problem was overcome and nominal observations resumed on July 10. Additionally, regular gaps of a few days through the whole mission's lifetime occur during the SOHO 'keyhole periods' (Robbrecht et al. 2009).

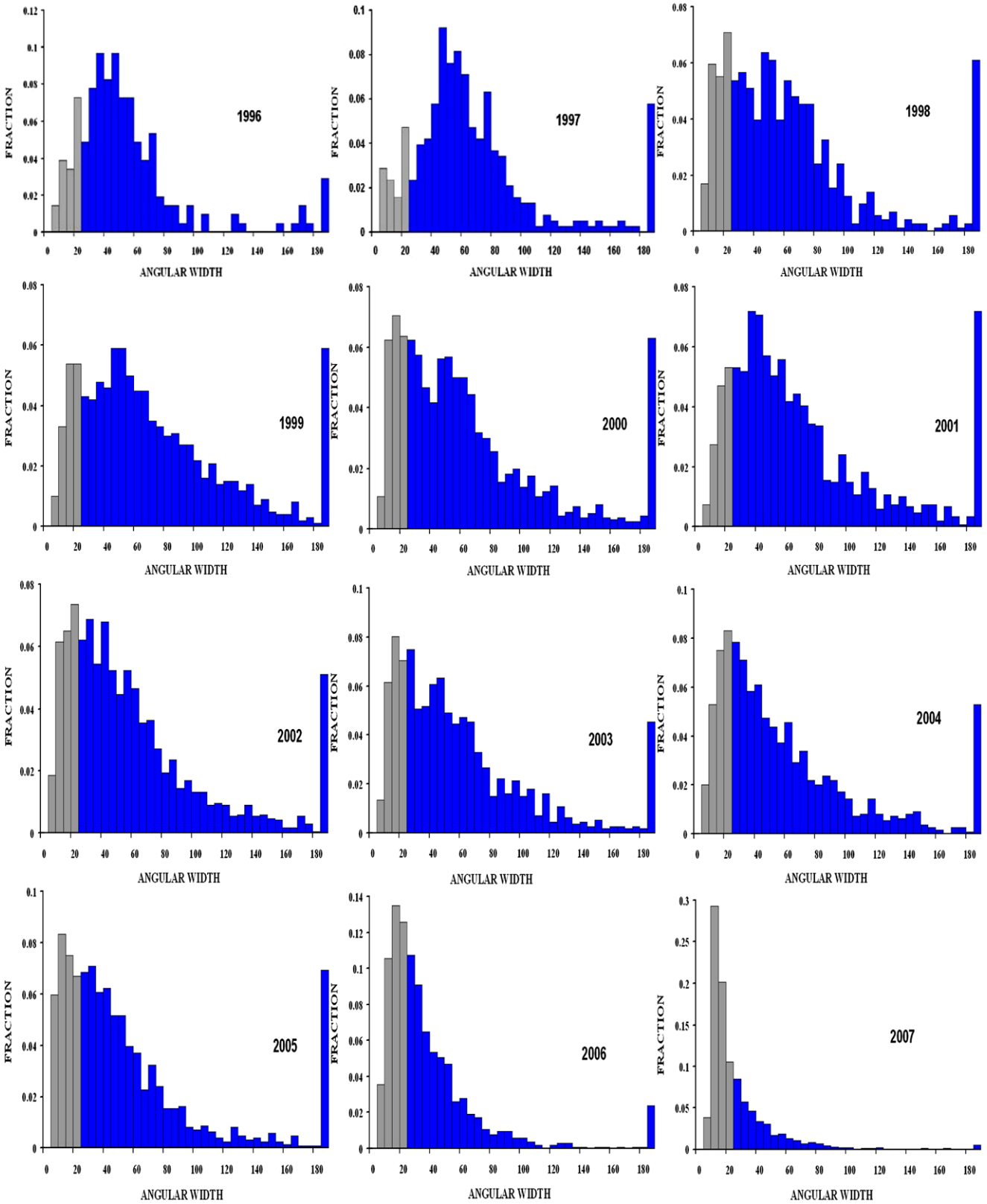

Fig. 1 Yearly width distribution of narrow (*light bars*) and normal (*dark bars*) CMEs from 1996–2007. The fractions along the *y*-axis indicate the number of CMEs with a given angular width divided by the total number of CMEs

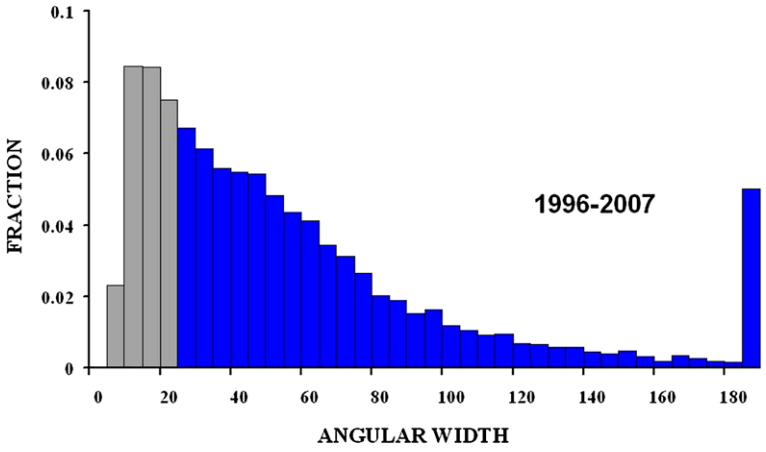

Fig. 2 Total distribution of widths of narrow (*light bars*) and normal (*dark bars*) CMEs from 1996–2007. The fractions in this figure have similar meaning as in Fig. 1

From Jan. 1996 to Dec. 2007, more than 12000 CMEs have been observed by SOHO/LASCO, which have a large range of angular widths. We define a narrow CME as one whose measurable apparent angular width is 20° or less, which is different from previous studies (Gilbert et al. 2001; Yashiro et al. 2003). Narrow CMEs are commonly referred to as "jets" which usually have ill-defined fronts but well defined sides (Burkepile and St. Cyr 1993).

The CME data used in this study have been taken from the catalogue maintained by the Centre for Solar Physics and Space Weather (CSPSW) (http://cdaw.gsfc.nasa.gov/CME_list). The online catalogue contains almost all major CMEs detected by the LASCO C2 and C3 coronagraphs. St. Cyr et al. (2000) have suggested that duty cycle correction may not be necessary for the LASCO data.

3 Properties of narrow CMEs

The key properties of narrow CMEs studied by us are width, speed, latitude, acceleration, and occurrence rate. Each topic is described in the following individual subsections:

3.1 Width distribution

CME width is measured as the position angle extent in the sky plane. For CMEs originating from close to the limb, the measured width is likely to be the true width. For CMEs located further away from the limb, the measured width is likely to be an overestimate as the calculations of Gilbert et al. (2001) show quite clearly. Many CMEs show an increase in width as they move out, so measurements are made when the width appears to approach a constant value. The yearly distributions of angular widths are shown in Fig. 1 from 1996–2007. The last bin in each plot seen in Fig. 1 includes all CMEs with widths $> 180°$. During the 1996–1997 solar minimum the shape of the distributions were simple and had peaks at $\sim 45°$. During 1998–1999 bi-model distributions were found with peaks located at $\sim 20°$ and 45°, whereas during 2000 the bi-model distributions were found with peaks located at $\sim 15°$ and 45°. During solar maximum 2002–2004 bi-model distributions were found again but with the peaks at different locations. In the final phase of the 2005–2007 solar minimum, it is clear that the peaks exist near $\sim 10°$ and in 2005 bi-model distributions was found with peaks located at $\sim 10°$ and 30° with clearly no bi-model distribution seen in 2006–2007. The histogram of all CMEs from year 1996–2007 in Fig. 2 shows a peak between $\sim 15°$ and 25°.

3.2 Speed distribution

Mass motion is a basic characteristic of CMEs and quantified by their speeds. Coronagraphs obtain images with a preset time cadence, and when a CME occurs, the leading edge moves to a greater heliocentric distance. On measuring the heliocentric distance of the leading edge of a CME in each LASCO image, one obtains CME height as a function of time. Height-time measurements are made in the sky plane, so all of the derived parameters such as speed etc. are the lower limits to the actual values (Gopalswamy 2006). The height-time plots are then fitted to first order polynomials which give an average speed within the LASCO field of view. The quadratic fit to the height-time plot gives constant acceleration which is an approximation because the acceleration may change with time (Gopalswamy 2006; Mittal and Narain 2009).

Figure 3 exhibits yearly speed distribution of narrow (light bars) and normal (dark bars) CMEs from 1996 to 2007. In Fig. 4 we have the histogram of speed distribution of **all** narrow (light bars) and normal (dark bars) CMEs observed during the period 1996–2007.

Table 1 summarizes the annual variation of the median (average) speeds of narrow and normal CMEs. A solar cycle variation is clearly seen. The median (average) speeds

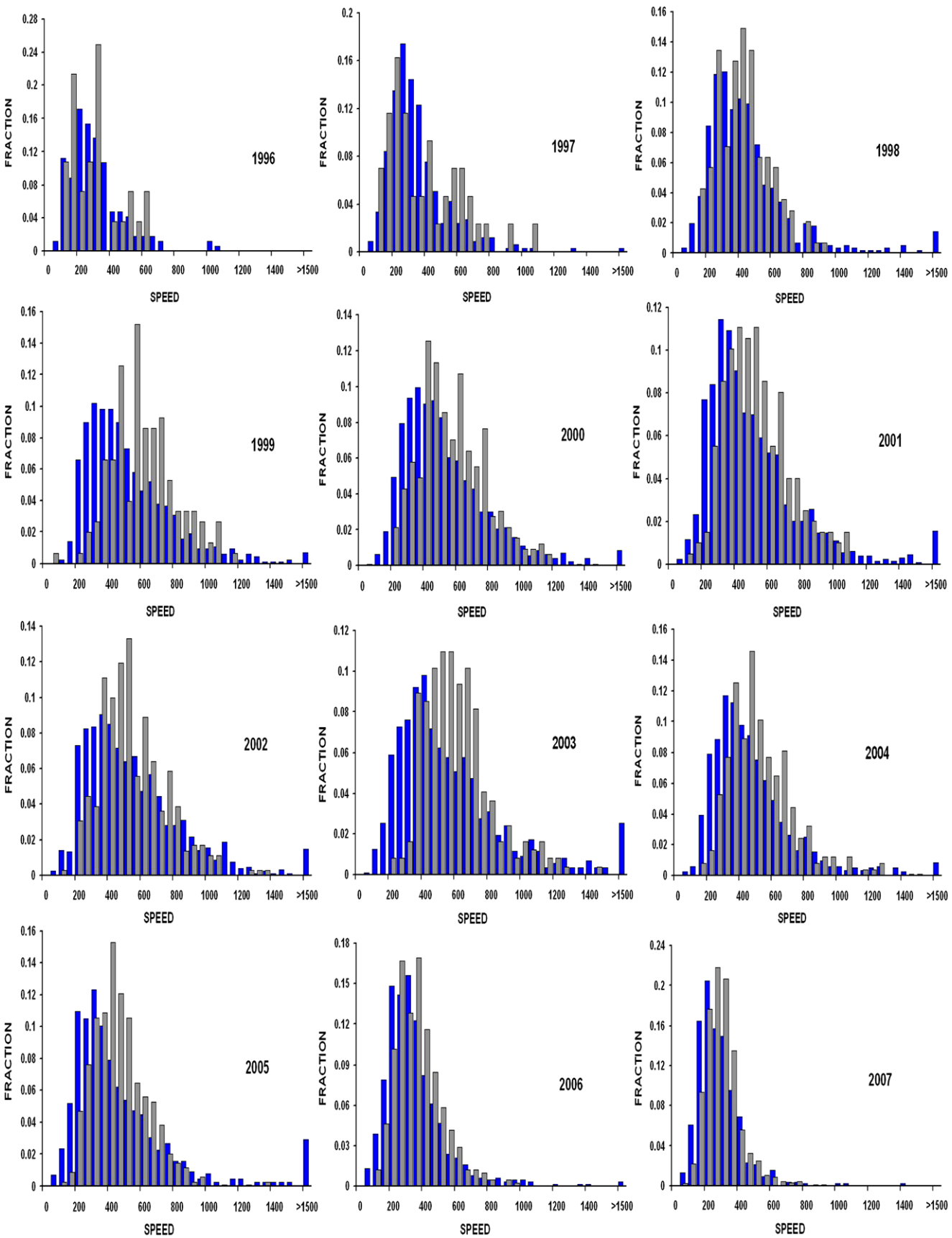

Fig. 3 Yearly speed distribution of narrow (*light bars*) and normal (*dark bars*) CMEs during 1996–2007. The last bin in each plot consists of all CMEs with speeds greater than 1500 km/s. The fraction along *y*-axis gives the fractional number of CMEs

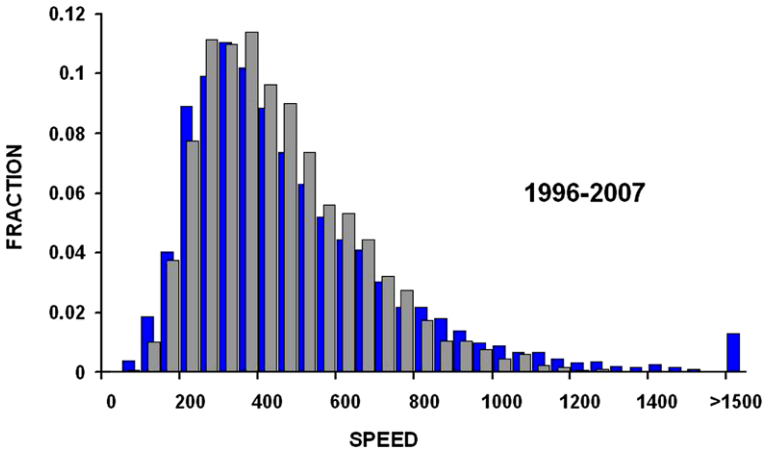

Fig. 4 Histogram shows the speed distribution of **all** narrow (*light bars*) and **all** normal (*dark bars*) CMEs during 1996–2007. The individual bars indicate the fraction of CMEs in a given speed range

Table 1 Speed (in km/s) of narrow and normal CMEs

Year	Narrow CMEs		Normal CMEs	
	Median	Average	Median	Average
1996	246	268	237	270
1997	277	348	272	316
1998	372	387	357	420
1999	550	575	415	480
2000	508	530	431	493
2001	463	484	391	471
2002	470	506	440	509
2003	538	570	445	536
2004	438	481	377	438
2005	400	424	335	440
2006	310	332	275	315
2007	248	262	215	242

during solar minimum (1996–1998, 2005–2007) were 309 (337) km/s for narrow CMEs and 282 (334) km/s for normal CMEs. The median speed of narrow CMEs is slightly higher than that of normal CMEs during solar minimum. In contrast, during solar maximum (1999–2004), the median (average) speeds were 495 (524) km/s for narrow CMEs and 416 (488) km/s for normal CMEs. Therefore, the median (average) speed of narrow CMEs is appreciably higher than that of normal CMEs during solar maximum.

The median (average) speed during (1996–2007) is 368 (409) km/s for narrow CMEs and 370 (445) km/s for normal CMEs. Figures 3 and 4 show the speed distribution from 1996–2007 for narrow (light bars) and normal (dark bars) CMEs. The CME fraction is shown per 50 km/s step. It is clear from the figures that the speed of narrow and normal CMEs increased towards solar maximum. For some CMEs, SOHO/LASCO is unable to measure CME speeds, therefore the number of events decreased compared to that used in the width distribution.

3.3 Latitude distribution

The latitudinal distribution of CMEs depends on the distribution of closed magnetic field regions on the solar surface. The CME latitude is obtained from the central position angle of the CME under the assumption that CMEs propagate radially away from the solar source region (Hundhausen 1993; Gopalswamy et al. 2003). This assumption may not be valid during solar minimum periods when the CME path may be controlled by the global dipolar field of the Sun.

Figures 5 and 6 show the distributions of apparent latitude from 1996–2007 for narrow (light bars) and normal (dark bars) CMEs. During solar minimum almost all CMEs occurred in the equatorial regions in the latitude range $\pm 20°$.

In 1998 the distributions for both narrow and normal CMEs grew broader in their latitudinal extents. During solar maximum (1999–2004) narrow CMEs appeared at all latitudes, similar to that found for normal CMEs. The distributions for both narrow and normal CMEs were consistent with the distribution of streamers. No significant differences were found between narrow and normal CMEs in their latitudinal distribution. It is clear from the figures that the ejections of both narrow and normal CMEs are equally distributed at all latitudes.

3.4 Acceleration distribution

All CMEs have positive acceleration as they first lift off from rest. Figures 7 and 8 show the acceleration distribution from 1996–2007 for narrow (light bars) and normal (dark bars) CMEs. The fractions in each 5 km/s^2 interval are plotted. It is clear from Figs. 7 and 8 that acceleration is biased towards deceleration. During solar minimum narrow CMEs and normal CMEs are mostly biased towards deceleration. During solar maximum narrow and normal CMEs both are also biased towards deceleration, but a small portion of both the narrow and normal CMEs do move with positive acceleration.

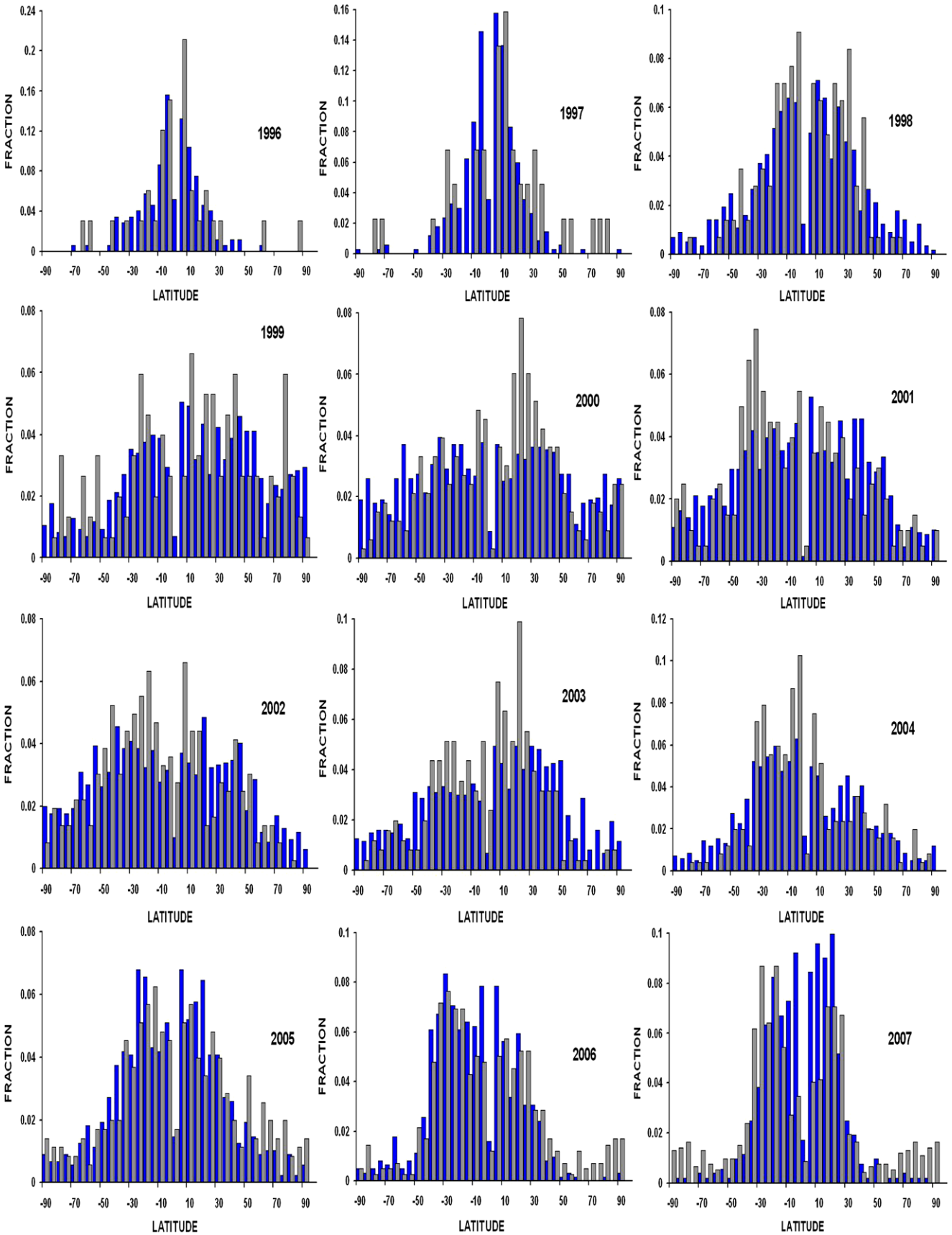

Fig. 5 Yearly north-south latitude distribution of narrow (*light bars*) and normal (*dark bars*) CMEs during 1996–2007. The fractions along the *y*-axis in the individual plots indicate the number of CMEs having a given latitude divided by the total number of CMEs

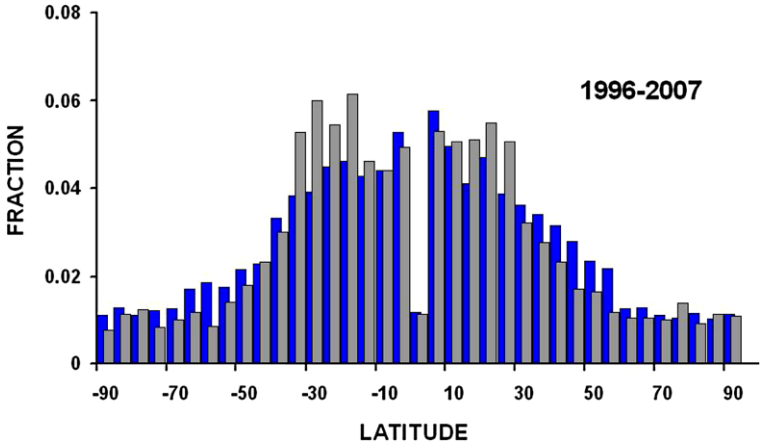

Fig. 6 Histogram shows the latitude distribution of **all** narrow (*light bars*) and **all** normal (*dark bars*) CMEs from 1996–2007. The fractions along *y*-axis in the figure give the fractional number of CMEs having given latitude

Actually, the normal CMEs seem to have a more normal distribution (with perhaps a slight shift towards deceleration), while narrow ones seem to be distinctly skewed towards deceleration because fast CMEs (speed > solar wind speed) predominantly decelerated within the LASCO field of view and deceleration must be due to drag (Gopalswamy et al. 2001) because the propelling forces fade out at heights below $\sim 4R_S$ (Chen and Krall 2003).

3.5 Occurrence rate of narrow CMEs

Figure 9 exhibits the daily occurrence rate of narrow and normal CMEs along with the monthly smoothed sunspot number for the interval 1996–2007. The CME occurrence rate is determined by taking the total number of CMEs that occurred during each Carrington Rotation (CR) from 1996–2007 and dividing by the CR period of 27.3 days. The rate of narrow CMEs keeps increasing towards the decline phase of solar cycle 23 similar to normal CMEs. The daily CME occurrence rate ranges from less than 0.1 to ~ 3.5 for narrow CMEs, while the rate of normal CMEs ranges from less than 0.5 to ~ 5.5. The CME rate in the declining phase remains nearly constant between years 2004–2007. During years 2004–2007 the rate of CME is high in comparison to sunspot number. This does not necessarily mean that these sunspots are more active, it could be due to more CME eruptions from non-sunspot regions. For convenience the annual occurrence rate is exhibited in Table 2.

It seems that the narrow CME occurrence rate is low during minimum (1996–1997). It then picks up in 1998 and remains almost constant thereafter until the beginning of 2006. The narrow CME occurrence rate suddenly increases in 2007 to exceed the occurrence rate of normal CMEs (cf. Fig. 9). This behaviour is quite different from that observed in 1996–2006 and is a new result.

A comparison of occurrence rate for narrow CMEs (with width $\leq 30°$) using the CDAW and CACTus catalogues by Yashiro et al. (2008) shows that there is appreciable difference between the rates. Since the CACTus catalogue follows the sunspot number for solar cycle variation of CME rate but CDAW does not, the CDAW catalogue might have missed some narrow CMEs during maximum phase of the cycle because they occurred just after a halo event. In fact, Robbrecht et al. (2009) show that nearly half of the CMEs detected by CACTus are narrow CMEs.

4 Discussion and conclusions

We investigated 3464 narrow CMEs (having widths $\leq 20°$) to compare with 9517 normal (widths $> 20°$) CMEs observed during the period 1996–2007, and arrived at the following results:

1. A majority of the narrow CMEs have widths in between 10° and 20°. The corresponding widths for normal CMEs lie in the range 25°–45° (cf. Fig. 1).
2. Most of the narrow CMEs have speeds in the range of 200–500 km/s. The corresponding speeds for normal CMEs lie in the range of 200–400 km/s (cf. Fig. 3). The maximum speed of narrow CME (1425 km/s) is much smaller than that of normal CME (3387 km/s). The population of narrow CMEs declines sharply at speeds greater than 700 km/s, whereas the distribution of normal CMEs has a high speed tail with declining population.
3. Most of the narrow CMEs have latitude in the range $-20°$ to $+20°$. The latitudes of a majority of normal CMEs also lie in the same range (cf. Fig. 5). Narrow CMEs are ejected from equatorial regions during solar minimum, while during solar maximum they originated from all latitudes, similar to normal CMEs.
4. The major population of narrow CMEs has acceleration in the range -15 to $+5$ km/s^2. The corresponding accelerations of the majority of normal CMEs is about

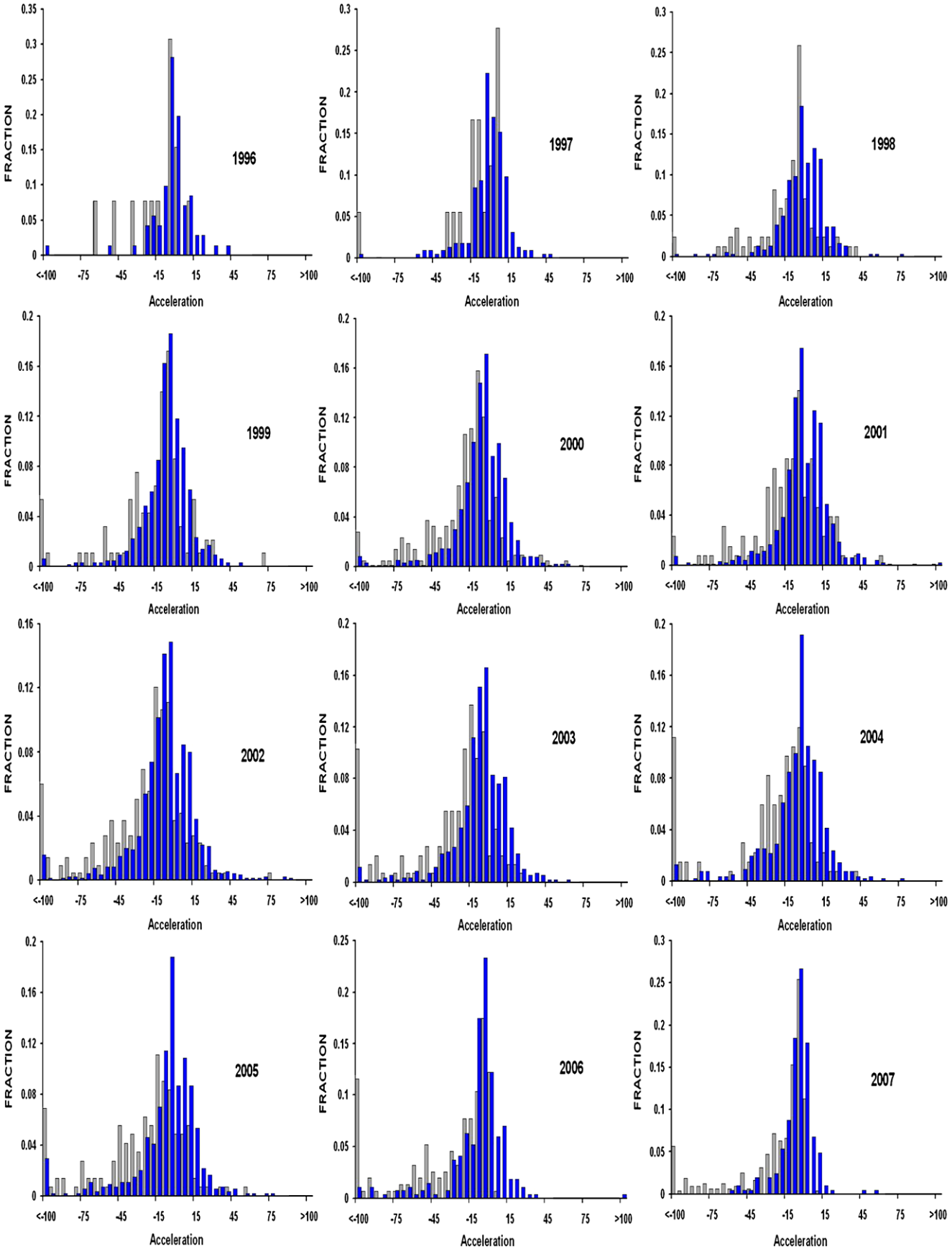

Fig. 7 Year-wise distribution of acceleration of narrow (*light bars*) and normal (*dark bars*) CMEs during 1996–2007. The fractions along *y*-axis in the figure give the fractional number of CMEs having given acceleration

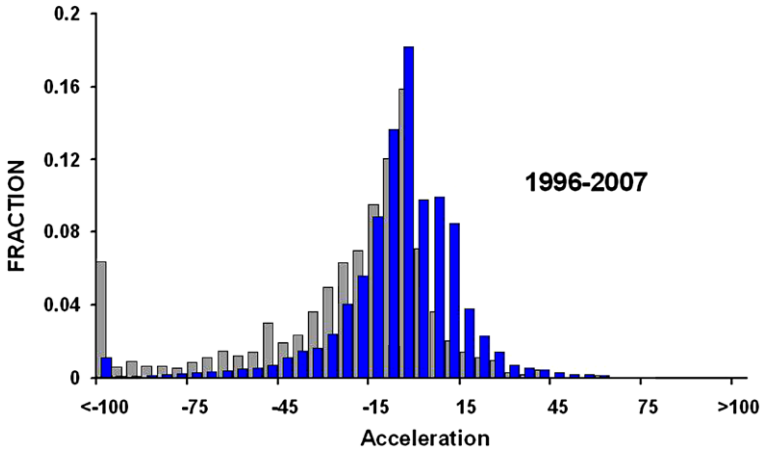

Fig. 8 Histogram of acceleration of **all** narrow (*light bars*) and **all** normal (*dark bars*) CMEs from 1996–2007 showing clear bias towards deceleration. The fractions along *y*-axis give the number of CMEs with a given acceleration divided by the total number of CMEs

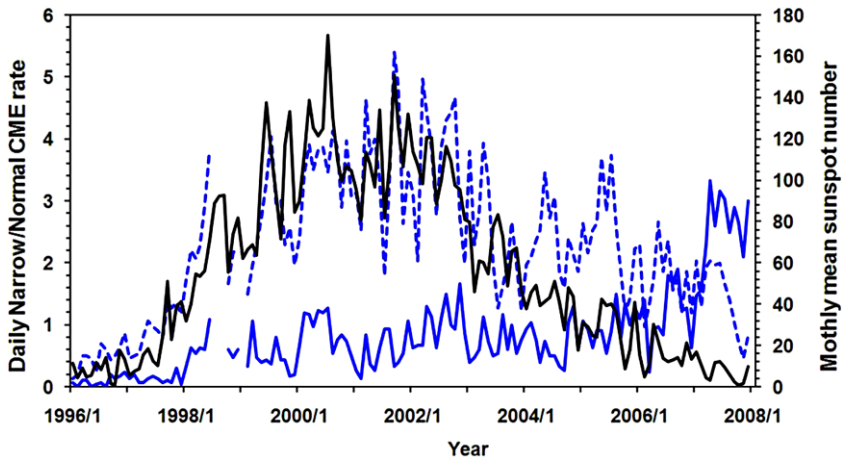

Fig. 9 Daily narrow and normal CME occurrence rate and monthly mean sunspot numbers. *Black solid line* represents monthly mean sunspot numbers; *blue solid line* shows narrow CMEs and *blue dotted line* represents normal CMEs. The discontinuity in curves is due to operation failure of SOHO/LASCO

Table 2 Annual occurrence rate of narrow and normal CMEs derived from LASCO for solar cycle 23

Year	1996	1997	1998	1999	2000	2001	2002	2003	2004	2005	2006	2007
Narrow CME	0.09	0.12	0.56	0.46	0.91	0.55	0.99	0.69	0.69	0.97	1.15	2.52
Normal CME	0.47	0.92	2.2	2.58	3.48	3.52	3.55	2.38	2.31	2.42	1.71	1.43

-5 km/s^2. Thus narrow CMEs seem to be distinctly skewed towards deceleration. Figure 8 shows a clear difference between the acceleration of narrow versus normal CMEs.

5. Whereas the occurrence rate of normal CMEs roughly follows the sunspot number variation (cf. Fig. 9), that of narrow CMEs remains almost constant from 1996–2006 and increases suddenly in 2007, as is clear from Table 2.

We may, therefore, conclude that there are some differences between the narrow and normal CMEs; in disagreement with the previous studies (Gilbert et al. 2001; Yashiro et al. 2003).

Acknowledgements We are thankful to Meerut College authorities for their help and encouragement. Authors are also thankful to IUCAA, Pune and HRI, Allahabad for financial assistance. We are highly grateful to N. Gopalswamy, N. Srivastava, P. Subramanian, P.K. Manoharan and A.K. Kembhavi for many helpful correspondences. The CME catalog is generated and maintained at the CDAW Data Center by NASA and The Catholic University of America in cooperation with the Naval Research Laboratory. SOHO is a project of international cooperation between ESA and NASA. The authors would like to thank for the excellent LASCO-CME catalogue, which includes supportive data—the back-bone of our paper. The authors are very much grateful to the learned referees for improving the manuscript through their enlightening comments.

References

Burkepile, J.T., St. Cyr, O.C.: A Revised and Expanded Catalogue of Mass Ejections Observed by the SMM Coronagraph, p. 181. NCAR, Boulder (1993) (NCAR-TN-369 + STR)

Chen, J., Krall, J.: J. Geophys. Res. **108**(A11), 1410 (2003)

Crifo, F., Picat, J.P., Cailloux, M.: Sol. Phys. **83**, 143 (1983)

Gilbert, H.R., Serex, E.C., Holzer, T.E., MacQueen, R.M., McIntosh, P.S.: Astrophys. J. **550**, 1093 (2001)

Gopalswamy, N.: In: Poletto, G., Suess, S. (eds.) The Sun and the Heliosphere as an Integrated System, ASSL series, p. 201. Kluwer, Boston (2004)

Gopalswamy, N.: J. Astrophys. Astron. **27**, 243 (2006)

Gopalswamy, N., Lara, A., Lepping, R.P., Kaiser, M.L., Berdichevsky, D., St. Cyr, O.C.: Geophys. Res. Lett. **27**, 145 (2000)

Gopalswamy, N., Lara, A., Yashiro, S., Kaiser, M.L., Howard, R.A.: J. Geophys. Res. **106**, 29107 (2001)

Gopalswamy, N., Yashiro, S., Michalek, G., Kaiser, M.L., Howard, R.A., Reames, D.V., Leske, R., von Rosenvinge, T.: Astrophys. J. **572**, L103 (2002)

Gopalswamy, N., Shimojo, M., Lu, W., Yashiro, S., Shibasaki, K., Howard, R.A.: Astrophys. J. **586**, 562 (2003)

Gopalswamy, N., Yashiro, S., Michalek, G., Stenborg, G., Vourlidas, A., Freeland, S., Howard, R.A.: Earth Moon Planets **104**(1), 295 (2009)

Howard, R.A., Sheeley, N.R. Jr., Michels, D.J., Koomen, M.J.: J. Geophys. Res. **90**, 8173 (1985)

Hundhausen, A.J.: In: Pizzo, V.J., Holzer, T.E., Sime, D.G. (eds.) Proc. Sixth International Solar Wind Conferences, vol. 2, p. 181. NCAR, Boulder (1987) (NCAR-TN-306)

Hundhausen, A.J.: J. Geophys. Res. **98**, 13177 (1993)

Hundhausen, A.J., Burkepile, J.T., St. Cyr, O.C.: J. Geophys. Res. **99**, 6543 (1994)

Illing, R.M.E., Hundhausen, A.J.: J. Geophys. Res. **91**, 10951 (1986)

Kahler, S.W., Reames, D.V., Sheeley, N.R. Jr.: Astrophys. J. **562**, 558 (2001)

Mittal, N., Narain, U.: New Astron. **14**(3), 341 (2009)

Mittal, N., Sharma, J., Tomar, V., Narain, U.: Planet. Space Sci. **57**(1), 53 (2009)

Munro, R.H., Sime, D.G.: Sol. Phys. **97**, 191 (1985)

Robbrecht, E., Berghmans, D., Van Der Linden, R.A.M.: Astrophys. J. **691**, 1222 (2009)

St. Cyr, O.C., et al.: J. Geophys. Res. **105**, 18169 (2000)

St. Cyr, O.C., Burkepile, J.T.: A catalogue of mass ejections observed by the SMM coronagraph, p. 181. NCAR, Boulder (1990) (NCAR/TN-352 + STR)

Tousey, R.: Space Res. **13**, 713 (1973)

Wang, Y.-M., Sheeley, N.R. Jr.: Astrophys. J. **575**, 542 (2002)

Wang, Y.-M., Sheeley, N.R. Jr., Socker, D.G., Howard, R.A., Brueckner, G.E., Michels, D.J., Moses, D., St. Cyr, O.C., Llebaria, A., Delaboudiniere, J.-P.: Astrophys. J. **508**, 899 (1998)

Webb, D.F., Cliver, E.W., Crooker, N.U., St. Cyr, O.C., Thompson, B.J.: J. Geophys. Res. **105**, 7491 (2000)

Yashiro, S., Gopalswamy, N., Michalek, G., Howard, R.A.: Adv. Space Res. **32**(12), 2631 (2003)

Yashiro, S., Gopalswamy, N., Michalek, G., St. Cyr, O.C., Plunkett, S.P., Rich, N.B., Howard, R.A.: J. Geophys. Res. **109**, A07105 (2004)

Yashiro, S., Michalek, G., Gopalswamy, N.: Ann. Geophys. **26**, 3103 (2008)